Study on the Preparation of Degradable Polyester from Waste High-boiling-point Electrolyte

Kun YU[1], Zhihua DENG[1]*, Xiaolong LI[2], Shen WANG[2], Haiyue WANG[2]*

1. College of Ecology and Environment, Southwest Forestry University, Kunming 650224, China; 2. School of Petrochemical Engineering, Shenyang University of Technology, Liaoyang 111003, China

Abstract In order to recover propylene carbonate (PC) from waste lithium-ion battery electrolyte, the electrolyte was coupled with dimethyl succinate (DMSu) to prepare degradable polyester PPS. To further enhance the performance of PPS, ethylene glycol (EG) was introduced to prepare copolyester PPSG, and the effects of the amount of added EG on the performance of copolyester were explored. The results show that the synthesized polyester was the target product. With the increase in the amount of added EG, the molecular weight of the copolyester gradually rose, but the glass transition temperature (T_g) of PPSG gradually decreased, and the degradation rate was significantly faster than that of PPS. Within 24 d, the mass loss rate of PPSG-30% reached 75.8%.

Key words Waste electrolyte; Polypropylene glycol succinate; Modification of ethylene glycol

DOI 10.19547/j.issn2152 - 3940.2025.03.014

In order to promote the control of plastic pollution in China, the state has introduced a series of policies and laws. In 2019, to solve the issue of plastic pollution, the state called for the promotion of degradable alternative products. In 2020, relevant state departments issued opinions, such as prohibiting or restricting certain plastic products, promoting degradable products, and standardizing recycling and high-value utilization[1].

The carbonate ester in the electrolyte of waste lithium batteries is a highly potential chemical raw material[2-3]. In low-boiling-point electrolyte, dimethyl carbonate (DMC), diethyl carbonate (DEC), and methyl ethyl carbonate (EMC) can all participate in polyester synthesis. In high-boiling-point electrolyte, ethylene carbonate (EC) and propylene carbonate (PC) have high chemical reactivity, and can also be used as monomer materials for polyester synthesis. Therefore, recycling the waste electrolyte and synthesizing degradable polyester can not only realize the high-value utilization of the waste electrolyte, but also provides a new approach for the preparation of degradable polyester[4-7].

In this paper, polyphenylene sulfide (PPS) was prepared by the coupling reaction of high-boiling-point electrolyte PC and DMSu[8-12]. The core reaction mechanism of the synthesis of polyester by the two was the ester exchange reaction. However, due to the large steric hindress of THE ring-opening of PC, the performance of the prepared PPS needs to be optimized. Therefore, PPSG was prepared by adding a third monomer ethylene glycol (EG), aiming to improve the comprehensive performance of PPS.

1 Materials and methods

1.1 Materials and instruments The main experimental reagents are as follows: lithium-ion battery electrolyte (industrial grade) was purchased from Suzhou Dingcheng New Energy Technology Co., Ltd.; dibutyltin oxide (AR grade), dimethyl succinate (DMSu, AR grade), propylene carbonate (PC, AR grade), ethylene glycol (EG, AR grade), dichloromethane (AR grade) were brought from Aladdin; Fourier transform infrared spectrometer (Magna-IR750) was purchased from American Nicolet Instrument Corporation; nuclear magnetic resonance spectrometer (Bruker 400M AVIII) was provided by German Bruker Company; differential scanning calorimeter (DSC822e) was offered by Mettler - Toledo of Switzerland.

1.2 Synthesis and preparation of degradable polyester PPS and its copolyester PPSG The synthesis reaction of degradable polyester PPS is carried out in two steps, and the reaction process is shown in Fig. 1.

Step 1 (transesterification reaction): Firstly, DMSu and PC recovered from the waste electrolyte were weighed according to a molar ratio of PC : DMSu = 1 : 1. EG was used as the third monomer for copolymerization. Four groups of EG with different contents were set up to synthesize copolyester PPSG, where the molar ratio of PC to EG was 10 : 0, 9 : 1, 8 : 2, and 7 : 3, respectively, and the corresponding products were respectively recorded as PPS, PPSG-10, PPSG-20, and PPSG-30. Afterwards, the raw materials were put into 250 mL four-necker flasks, to which a certain amount of catalyst (accounting for 1% of the total mass of the raw materials) was added. The airtightness of the device was checked. Nitrogen was slowly input into the system to expel all the air in the device, and then the condensate water was turned on. The temperature was enhanced slowly to 210 ℃ by heating. The ester exchange reaction was conducted under normal pressure. The reaction ended when the temperature at the top of the reaction column dropped below 60 ℃. Finally, the distillate was collected

Received: April 19, 2025 Accepted: May 26, 2025

* Corresponding author.

and characterized.

Step 2 (polycondensation reaction): after the transesterification reaction was completed, the system temperature was reduced to 160 ℃. Then, the vacuum pump was started to reduce the pressure, and the reaction temperature was slowly increased to 210 ℃. Under vacuum conditions, the reaction continued for 5 h to increase the molecular weight of the polyester. After the reaction was completed, the product was dissolved in dichloromethane, and then the dissolved liquid was dropped into the excess methanol to precipitate the polymer. It was dried in a vacuum drying oven at 40 ℃ for 24 h to obtain the final polyester product.

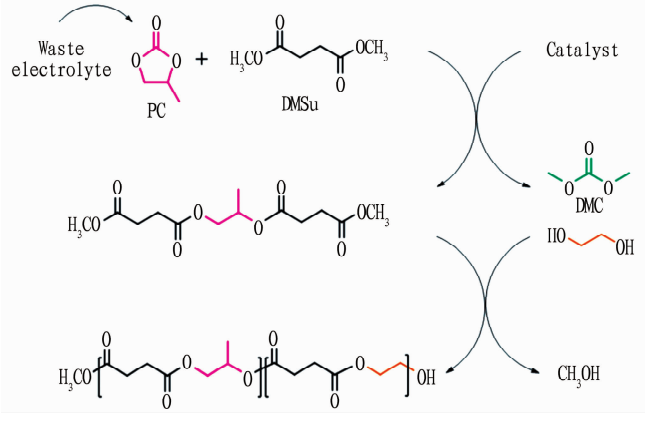

Fig. 1 Schematic diagram of the synthesis of PPSG by the coupled reaction method

2 Results and analysis

2.1 FTIR The infrared structures of polyester PPS and copolyester PPSG were characterized, and the infrared spectra are shown in Fig. 2. It can be seen from the figure that the absorption peak at 2 966 cm^{-1} was the characteristic peak of the C – H stretching vibration of methyl and methylene groups in the carbon chain, and the strong absorption peak at 1 728 cm^{-1} was the characteristic peak of the stretching vibration of carbonyl group C = O; the strong absorption peak at 1 142 cm^{-1} was the characteristic peak of the stretching vibration of C – O – C bond, and the vibration peak at 763 cm^{-1} corresponded to the C – H bending vibration generated when the succinic acid chain segment was connected to two methylene groups in the ethylene glycol chain segment. It is preliminarily proved that the structure of the synthesized PPS and its copolyester PPSG was correct.

2.2 ^{1}H NMR analysis The molecular formula of copolyester PPSG contains two repetitive structural units (A and B), as shown in Fig. 3. The nuclear magnetic resonance hydrogen spectra of PPS and its copolyester PPSG-30% samples are shown in Fig. 4.

The molecular chain structure of PPS and its copolyester PPSG-30% was characterized by nuclear magnetic resonance hydrogen spectroscopy (^{1}H NMR). The results show that there were five characteristic peaks of H (a, b, c, d, and e) in the spectrum of PPSG-30%. The integral area ratio and splitting mode of each peak were analyzed. It is concluded that the five peaks of H corresponded respectively to the five characteristic peaks of H in different environments in the figure.

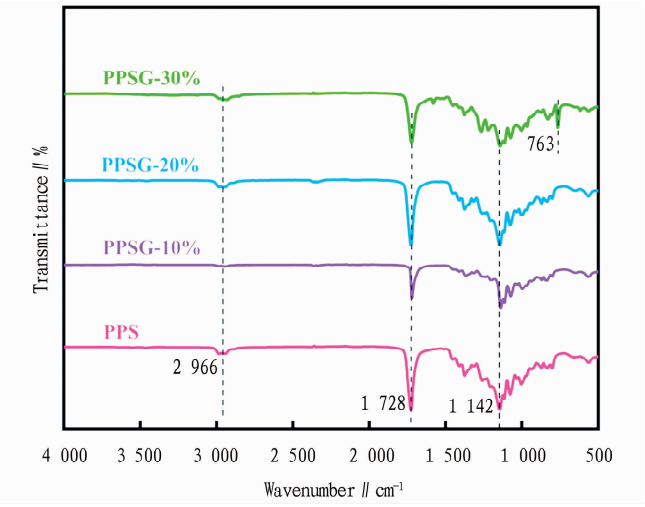

Fig. 2 FT-IR spectra of PPS and PPSG

It can be seen from the figure that δ = 7.26 corresponded to the solvent deuterated chloroform; δ = 2.63 represented the chemical shift of hydrogen at position a on the methylene group adjacent to the ester group in the succinic acid fragment; δ = 1.29 meant the chemical shift of hydrogen at position b on the side methyl group in the propylene glycol fragment in the repetitive structural unit A; δ = 3.68 was the chemical shift of hydrogen at position c on the methylene group connected to propylene glycol and succinic acid; δ = 5.13 represents the chemical shift of hydrogen at position d on the methine group connected to the side methyl group on propylene glycol; δ = 4.20 represents the chemical shift of hydrogen at position e on the methylene group in the ethylene glycol fragment in the repetitive structural unit B. According to the analysis results of infrared spectra, it is further verified that the structure of the synthesized PPS and its copolyester PPSG was correct.

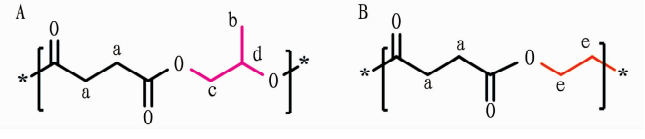

Fig. 3 Two structural units of PPSG copolyester

2.3 Analysis of molecular weight The intrinsic viscosity and viscosity-average molecular weight of the synthesized PPS and copolyester PPSG samples were tested by the dilute solution viscosity method. The results are shown in Table 1.

From the table, it can be seen that with the increase of EG, the molecular weight of PPS and its copolyester PPSG both rose, and the intrinsic viscosity [η] first increased and then decreased. When EG content was low, the terminal hydroxyl group of EG as a highly active diol monomer could promote the ester exchange reaction, increase the polymerization degree of the reaction, accelerate the growth of molecular chains, and increase the molecular weight of the PPS system, thereby leading to an increase in intrinsic viscosity. With the further increase of EG content, the proportion of amorphous phase in the PPS system rose, and the regularity of mo-

lecular chains declined, resulting in an increase in short chains and a decrease in the overall molecular weight, which in turn led to a reduction in intrinsic viscosity.

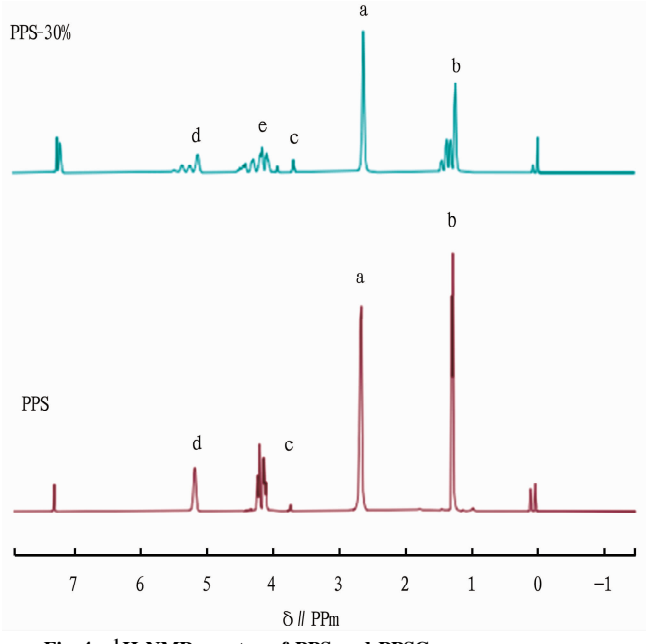

Fig. 4 ^{1}H-NMR spectra of PPS and PPSG

Table 1 Intrinsic viscosity and viscosity-average molecular weight of PPS and PPSG

PPS or PPSG	Intrinsic viscosity[η] // dL/g	M_η // g/mol
PPS	0.42	21 088
PPSG-10%	0.50	26 607
PPSG-20%	0.47	24 500
PPSG-30%	0.46	23 808

2.4 Analysis of the glass transition and melting transformation behaviors of EG-modified PPS copolyester The glass transition and melting transformation behaviors of PPS and its copolyester PPSG were tested by DSC, and the results are shown in Fig. 5. The results reveal that with the gradual increase of EG content, the glass transition temperature (T_g) gradually decreased from −15.6 to −21.4 ℃. Due to the short chain structure of EG, the flexibility of molecular chain segments increased, and the hydrogen bond interaction between molecules weakened, thereby reducing the interaction force and bulk density of molecular chains, and ultimately leading to a significant decrease in T_g. In addition, the asymmetry and lower molecular rigidity of EG further enhanced the free movement ability of the chain segments, increasing the proportion of amorphous phases in the system and thereby affecting the thermodynamic properties of the polymer. This is because the asymmetry and lower molecular rigidity of EG made the polymer chain segments more prone to movement, resulting in a decline in crystallization ability, crystallinity, and then melting temperature (T_m). The introduction of EG weakened the stability of the crystalline zone, made the crystalline structure of PPS more disordered, improved the flexibility of PPS, and enhanced the adaptability of the material in processing procedures such as injection molding, extrusion and film forming.

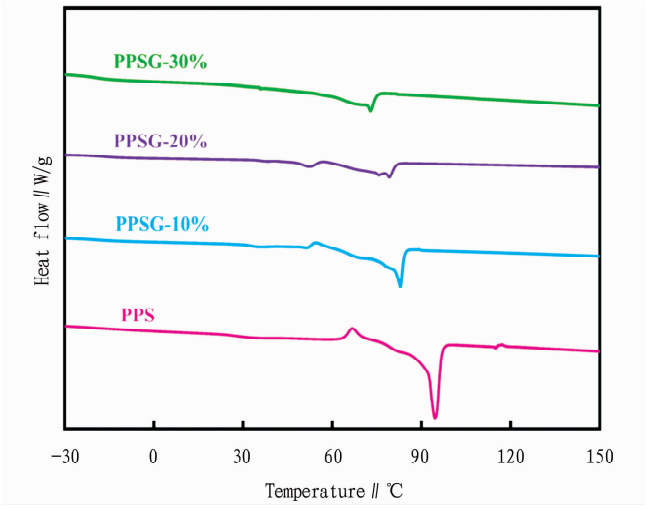

Fig. 5 Curves of glass transition and melting transition of PPS and PPSG

2.5 Analysis of the biodegradation performance of copolyester PPSG The biodegradation performance of PPS and its copolymer samples PPSG-10%, PPSG-20%, and PPSG-30% was tested, and the degradation curves are shown in Fig. 6. With the addition of ethylene glycol monomer, the degradation ability of PPSG was higher than that of polymer PPS. Moreover, the enzymatic degradation of the four polyesters was a relatively fast in the first 15 d, because the enzyme mainly acted on the material surface and amorphous regions, and more ester bonds of the polymer were exposed in the early stage of degradation. Since the 15th day, the degradation slowed down, because the remaining part was the crystalline region or the cross-linked region of the molecular chains, making it difficult for the enzyme to further penetrate.

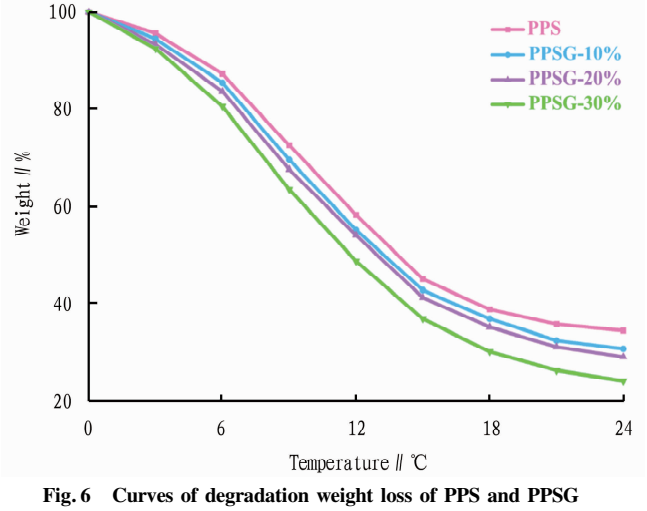

Fig. 6 Curves of degradation weight loss of PPS and PPSG

3 Conclusions

In this study, a new copolyester PPSG was prepared by adding a third monomer, ethylene glycol (EG), to the reaction

(To page 74)

[18] FAJARDO C, MORA M, FERNANDEZ I, *et al*. Cross effect of temperature, pH and free ammonia on autotrophic denitrification process with sulphide as electron donor[J]. Chemosphere, 2014, 97(2): 10 – 15.
[19] CUI YX, BISWAL BK, GUO G, *et al*. Biological nitrogen removal from wastewater using sulphur-driven autotrophic denitrification[J]. Applied Microbiology and Biotechnology, 2019, 103(15): 6023 – 6039.
[20] CLAUS G, KUTZNER HJ. Physiology and kinetics of autotrophic denitrification by *Thiobacillus denitrificans*[J]. Applied Microbiology and Biotechnology, 1985, 22(4): 283 – 288.
[21] CAPUA FD, AHORANTA SH, PAPIRIO S, *et al*. Impacts of sulfur source and temperature on sulfur-driven denitrification by pure and mixed cultures of *Thiobacillus*[J]. Process Biochemistry, 2016, 51(10): 1576 – 1584.
[22] YUAN Y, ZHOU WL, WANG H, *et al*. Study on sulfur-based autotrophic denitrification with different electron donors[J]. Environmental Science, 2013, 34(5): 10.
[23] ZHANG CX, GUO YK, DU HF, *et al*. Denitrification characteristics of a sulfur autotrophic denitrification reactor[J]. Journal of Hebei University of Science and Technology, 2016, 37(1): 6.
[24] WANG J, LU H, CHEN GH, *et al*. A novel sulfate reduction, autotrophic denitrification, nitrification integrated (SANI) process for saline wastewater treatment[J]. Water Research, 2009, 43(9): 2363 – 2372.
[25] LI J, ZHENG CJ, LIU J, *et al*. Effects of S^{2-}/NO_3^--N on sulfur autotrophic denitrification and anaerobic ammonia oxidation combined process for nitrogen and sulfur removal[J]. Research of Environmental Sciences, 2015, 28(7): 7.
[26] LIU C, LI W, LI X, *et al*. Nitrite accumulation in continuous-flow partial autotrophic denitrification reactor using sulfide as electron donor[J]. Bioresource Technology, 2017, 243: 1237 – 1240.
[27] CHEN C, ZHANG RC, XU XJ, *et al*. Enhanced performance of denitrifying sulfide removal process at high carbon to nitrogen ratios under micro-aerobic condition[J]. Bioresource Technology, 2017, 232: 417 – 422.
[28] DU FW. Research on deep nitrogen removal from wastewater by biological aerated filter and sulfur autotrophic denitrification filter[D]. Harbin: Harbin Institute of Technology, 2011.
[29] CHEN C, WANG A, REN N, *et al*. Enhancing denitrifying sulfide removal with functional strains under micro-aerobic condition[J]. Process Biochemistry, 2010, 45(6): 1007 – 1010.
[30] CHEN C, REN N, WANG A, *et al*. Enhanced performance of denitrifying sulfide removal process under micro-aerobic condition[J]. Journal of Hazardous Materials, 2010, 179(1 – 3): 1147 – 1151.
[31] CAMPOS JL, MOSQUERA-CORRAL A, SÁNCHEZ M, *et al*. Nitrification in saline wastewater with high ammonia concentration in an activated sludge unit[J]. Water Research, 2002, 36(10): 2555 – 2560.
[32] CHEN GH, WONG MT, OKABE S, *et al*. Dynamic response of nitrifying activated sludge batch culture to increased chloride concentration[J]. Water Research, 2003, 37(13): 3125 – 3135.
[33] ZHOU P. Research on the effects of acclimation methods on the biological nitrification and denitrification performance of saline wastewater[D]. Qingdao: Qingdao University of Science and Technology, 2010.
[34] LIU CS, ZHAO DF, MA WJ, *et al*. Denitrifying sulfide removal process on high-salinity wastewaters in the presence of *Halomonas* sp.[J]. Applied Microbiology and Biotechnology, 2016, 100(3): 1421 – 1426.
[35] YU H. Analysis of microbial community structure and function in synchronous desulfurization and denitrification process[D]. Harbin: Harbin Institute of Technology, 2014.
[36] FANG Y. Review of the metabolic characteristics of nitrate-reducing, sulfide-oxidizing bacteria and its environmental application[J]. Environmental Pollution & Control, 2015, 37(4): 5.
[37] ZHAO JN, LIU SY, SHAN YQ, *et al*. Rapid start-up and microbial community analysis of a sulfur autotrophic denitrification coupled anaerobic ammonia oxidation denitrification system[J]. Environmental Engineering, 2024, 42(6): 9 – 16.

(From page 70)

system of dimethyl succinate (DMSu) and propylene carbonate (PC). The results show that the structure of the prepared PPSG copolyester was correct. Moreover, with the addition of the third monomer EG, the glass transition temperature of the copolyester reduced from −15.6 to −21.4 ℃, and the melting temperature declined from 94.5 to 72.8 ℃. With the increase of the amount of added EG, the biodegradability of PPSG gradually was improved, and the degradation weight loss rate of PPSG-30% within 24 d reached 75.8%. Therefore, the comprehensive performance of copolyester PPSG prepared with EG as the third monomer was superior to the original polyester PPS.

References

[1] ZHAO XD. Study on the preparation of metal-based ionic liquids and catalytic synthesis of pes from EC and its properties[D]. Shenyang: Shenyang University of Technology, 2023.
[2] ZHENG S, CHEN T, FANG Y, *et al*. A review of cathode and electrolyte recovery from spent lithium-ion batteries: Recent technologies, processes and policies[J]. Resources Chemicals and Materials, 2024, 3(3): 188 – 229.
[3] PYO SH, PARK JH, CHANG TS, *et al*. Dimethyl carbonate as a green chemical[J]. Current Opinion in Green and Sustainable Chemistry, 2017, 5: 61 – 66.
[4] SHI G, WANG J, ZHANG S, *et al*. Green regeneration and high-value utilization technology of the electrolyte from spent lithium-ion batteries[J]. Separation and Purification Technology, 2024, 335: 126144.
[5] LU XF, FU Q, SUN Q, *et al*. Research progress on electrolyte recovery of spent lithium ion batteries[J]. Sustainable Mining and Metallurgy, 2023, 39(1): 75 – 79, 84.
[6] LI YG, HAN DZ, QI LJ. Recent research on pretreatment of waste lithium ion batteries and electrolyte recovery technology[J]. Inorganic Chemicals Industry, 2024, 56(2): 1 – 10.
[7] WANG QS, JIANG LH, YU Y, *et al*. Progress of enhancing the safety of lithium ion battery from the electrolyte aspect[J]. Nano Energy, 2019, 55: 93 – 114.
[8] ZHAO X, GUO L, XU T, *et al*. Preparation of biacidic tin-based ionic liquid catalysts and their application in catalyzing coupling reaction between ethylene carbonate and dimethyl succinate to synthesize poly(ethylene succinate)[J]. New Journal of Chemistry, 2022, 46(33): 15901 – 15910.
[9] ZHAO X, GUO L, XU T, *et al*. Preparation of Keggin-type monosubstituted polyoxometalate ionic liquid catalysts and their application in catalyzing the coupling reaction of ethylene carbonate and dimethyl succinate to synthesize poly(ethylene succinate)[J]. New Journal of Chemistry, 2022, 46(42): 20092 – 20101.
[10] LIU C, ZENG J B, LI S L, *et al*. Improvement of biocompatibility and biodegradability of poly(ethylene succinate) by incorporation of poly(ethylene glycol) segments[J]. Polymer, 2012, 53(2): 481 – 489.
[11] SUN Z, CHEN M, XIE G, *et al*. Synthesis and properties of biodegradable poly(ethylene succinate) containing two adjacent side methyl groups[J]. Polymer, 2023, 283: 126300.
[12] KUMAGAI S, IMADA M, HAYASHI S, *et al*. Synthesis and characterization of block copolymers consisting of poly(ethylene succinate) and poly(amino acid)s[J]. Polymer Degradation and Stability, 2025, 235: 111265.